Received: 14 February 2020 | Revised: 27 March 2020 | Accepted: 28 March 2020

DOI: 10.1111/dth.13362

Check for updates

DERMATOLOGIC THERAPY WILEY

ORIGINAL ARTICLE

Remodeling of collagen constituting interlobular septa of subcutaneous adipose tissue following microwaves application

Nicola Zerbinati[1] | Edoardo d'Este[2] | Aurora Farina[3] | Antonia I. Cornaglia[3] | Mohammad Jafferany[4] | Masa Golubovic[5] | Iva Binic[6] | Julia Sigova[7] | Nguyen Van Thuong[8] | Michael Tirant[8] | Federica Riva[3] | Marina Protasoni[1] | Raffaele Rauso[9] | Torello Lotti[10] | Alberto Calligaro[3]

[1]Department of Surgical and Morphological Sciences, University of Insubria, Varese, Italy

[2]Centro Medico Polispecialistico, Pavia, Italy

[3]Department of Public Health, Experimental and Forensic Medicine, Unit of Histology and Embryology, University of Pavia, Pavia, Italy

[4]Central Michigan University, Saginaw, Michigan

[5]Department of Dermatology, Clinical Center, University of Nis, Serbia

[6]Department of Psychiatry, Clinical Center, University of Nis, Serbia

[7]Department of Neonatology, Faculty of Continued Medical Education of Pirogov Russian National Research Medical University, Moscow, Russia

[8]Department of Dermatology, Hanoi Medical University, Hanoi, Vietnam

[9]Maxillofacial Surgery Unit, University of Campania "Luigi Vanvitelli", Naples, Italy

[10]Department of Dermatology, University of Rome G. Marconi, Rome, Italy

Correspondence
Mohammad Jafferany, Central Michigan University, Saginaw, MI.
Email: mjafferany@yahoo.com

Abstract

In this study, the application of a recently introduced device based on electromagnetic energy transfer by microwaves for fat reduction, permitted to study specifically the modifications of thick fibrous collagen interlobular septa in the subcutaneous adipose tissue, related to the formation of large clusters of adipocytes. The use of Picrosirius red staining associated with circularly polarized microscopy gave evidence of appreciable modifications of the fibrous connective tissue forming septa. Compact fibrotic bundles of collagen I forming interlobular septa appeared reduced or dissolved, in part substituted by the increase of more diffuse and finely reticular collagen III. Remodeling of fibrous collagen, which formed bridles involved in the appearance at the surface of the skin of dimpling/orange peer pattern typical of cellulite, was observed.

KEYWORDS

circularly polarized microscopy, collagen remodeling, fat reduction, microwave device, Picrosirius red

1 | INTRODUCTION

Many authors have presented theoretical and experimental papers using methods and devices with as objective the reduction of adipose tissue. Particular interesting is a recent paper[1] in which they have been considered the properties of some tissues related to the absorption of microwaves (MW) energy in different models, using equivalent phantoms and ex vivo measurements. The most part of experimental evaluations available in literature, related to fat reduction, have been performed in vitro conditions, which only in few cases could represent what and how happens in vivo, in the complex dynamics inside tissues and organs.

Recently, a new technology for the reduction of subcutaneous adipose tissue (SAT) has been developed with a noninvasive treatment by MW. The controlled electromagnetic energy transfer induces thermal modifications into SAT, starting molecular mechanisms with the result of fat reduction.[2]

The aim of this article is not to underline the effectiveness of the treatment as fat reduction already demonstrated,[2] but to give new morphological evidences of structural modifications of compact collagen constituting interlobular septa in the SAT. It is well known that cellulite, together any other possible cause, is structurally determined by highly compact fibrotic septa dividing large clusters of adipose

 © 2020 Wiley Periodicals LLC

tissue as tethered compartments, producing the typical dimpling/orange peel pattern.[3,4]

Our results demonstrate that compacted collagen fibers constituting fibrotic septa undergo to fragmentation and remodeling, starting few hours following MW treatment.

2 | METHODS

The study was conducted as University of Insubria, Varese, Italy. A controlled electromagnetic field (EMF) @2.45 GHz, perpendicularly applied to the skin, is selectively absorbed by the subdermal fat layer thanks to the dielectric properties of the different tissues (epidermis, dermis, fat) crossed by the applied EMF. The highly controlled emission of the EMF is able to establish a perfect coupling only in the presence of fat layer, due to the absorption characteristics of this tissue at the established frequency.

The applied noninvasive transcutaneous EMF (Coolwaves by Onda, DEKA, Florence, Italy) was applied in order to thermally induce adipocytes' damage. During the treatment, applying a transmitting handpiece on the surface of the skin, the EMF energy was delivered into the SAT of a Vietnamese pig (this study on the animal model was carried out in full compliance with international guidelines for safety and compliance with their use) with a 50.000 J total dose delivered in 7 minutes over a cutaneous area 15×15 cm^2. The handpiece used was maintained at the temperature of 5°C through a specific cooling system.

The experimental plan was designed on the basis of a single irradiation session for each skin region treated. Biopsy samples were collected and processed for light microscopy, owing to the following steps: T0 (before treatment, as control), T1 (immediately after treatment), T2 (1 hour following treatment), and T3 (6 hours following treatment).

Temperature monitoring was performed at the skin surface by a thermometric infrared camera vision system, and deeply, in the subdermal fat layer, by a sterile thermometric glass fiber. The temperature in the treated area was monitored in a safety range of 15°C to 25°C on epidermis, and of 47°C to 50°C in subcutaneous tissue.

At each time step (T0, T1, T2, T3), skin biopsy samples were immediately immersed in a 4% paraformaldehyde/sodium phosphate buffer solution for 24 hours and then processed (dehydration, paraffin embedding, and sectioning) for light microscopy.

Specific preparation of sections for light microscopy was made using a staining method based on Picrosirius red, a dye which not only stains specifically collagen fibers, but also enhances the collagen optical birefringence.[5-7] Picrosirius red was used as a solution 0.1% of Sirius red F3B in a saturated aqueous solution of picric acid for 1 hour at room temperature. The sections to be compared, all with the same thickness of 7 μm, were stained keeping the same time in the same dye solution. A faint staining with hematoxylin was also used for nuclei detection.

Picrosirius red staining does not exhaust its potentiality only as selective staining of collagen and enhancement of its birefringence, but using circularly polarized microscopy it permits the identification and differentiation of big bundles of collagen (mature) and smaller fibers and fibrils (newly formed) through a scale of colors. At the light microscope provided with an optical setting for circularly polarized light, Picrosirius red stained fibers can be differentiated through a scale of different colors. Birefringent structures (collagen fibers) in the connective tissue are highly visible not only as brilliant structures, but some of them appear Red/Orange and others appear Yellow/Green. In the scale of colors, Red/Orange structures are representing thick compacted collagen fibers of collagen I, while Yellow/Green are representing thin fibers of collagen III.[8]

On this basis, to the sections of the same thickness observed with circularly polarized light, it has been possible to apply a computerized morphometric analysis through a specific thresholding on the color scale, permitting the identification and the evaluation of thick collagen fibers (R/O mature, collagen I), and thin collagen fibers (Y/G immature, the most recently formed, collagen III). These last are expression of the remodeling of the extracellular matrix collagen components.

Microscopic observations were made at a light microscope Carl Zeiss Axiophot provided, for circular polarizing microscopy, with suitable filters in the condenser stage and in the microscope tube. Images were recorded through a digital 5 megapixel CCD camera Nikon DS-Fi2.

A computerized morphometric analysis was also performed, on the basis of 10 frame areas 2560×1920 sq pixels for each sample, using as the most reliable tool ImageJ (NIH, version 1.51a), a well-known software recognized as standard tool by international scientific community.

The following different steps used as ImageJ tools, and the operative sequence with related meanings are reported.

- *File open*.
- *Image*, *type RGB color*.
- *Adjust*, *color threshold*: The adjustment of *Hue*, *Saturation*, *Brightness* parameters permitted the interactive selection of the Red/Orange or Yellow/Green threshold values in order to have masks exactly superposed to the structures of interest to be saved in two different channels R/O and Y/G. The Hue upper value for Red/Orange must be separated by a well-defined cleft from the lower Hue value for Yellow/Green, in order to prevent superposition of data and a double evaluation into the two channels of the same structures.

  In this study, the values were:

  R/O Red/Orange channel: Hue 0 to 34, Saturation 106 to 255, Brightness 106 to 186.

  Y/G Yellow/Green channel: Hue 44 to 118, Saturation 106 to 255, Brightness 106 to 186.
- *Save as*: Red/Orange and Yellow/Green were saved as single images of the two different channels.

For a correct comparison of results, obtained from sections of the same thickness and stained at the same time and in the same staining solutions, the values of Hue, Saturation, Brightness thresholds were maintained the same for all the microscopic preparations compared.

In the following steps, each one of the analogic continuous tone images representing the two channels was converted into a digital one.

- *Image*, *type*, *8bit*.
- *Image*, *adjust*, *threshold*: it means to extract from each selected continuous tone image, a binary image. So the areas of interest corresponding to the defined channel masks (Red/Orange or Yellow/Green) are constituted by black pixels (signal) on a white background. These images are ready for the measurements.
- *Edit*, *selection*, *select all*.
- *Analyze*, *select particles*. Select the following parameters: Display results, Summarize, Add to Manager, In situ show. The area % occupied by Red/Orange and Yellow/Green fibers, respectively, in each one of the reference frames of 2560 × 1920 sq pixels was so obtained and registered for comparisons by statistical analysis.

2.1 | Statistical analysis

Statistical analysis of the measurements of Red/Orange and Yellow/Green collagen fibers at T0, T1, T2, and T3 was performed using an unpaired *t* test and the one-way analysis of variance. The significance level was set at $P < .01$.

3 | RESULTS

Controlled hyperthermia has been determined in the SAT, with effect on hypertrophic adipocytes, severe adipolysis with the active participation of monocytes and macrophages which remove adipocytes residuals. Following MW Onda treatment—at the same time of the expression of molecular mechanisms involving adipocytes and responsible of adipolysis—we have observed an involvement of the connective tissue constituting the interlobular septa, particularly evident on the thicker and fibrotic bundles of collagen fibers between bigger adipose lobules (Figure 1A,B). In Figure 2A, two microscopic fields of interlobular septa stained with Picrosirius red are represented, as observed at the circularly polarized light microscope. The same Figure 2A shows different colors in the different bands defined by

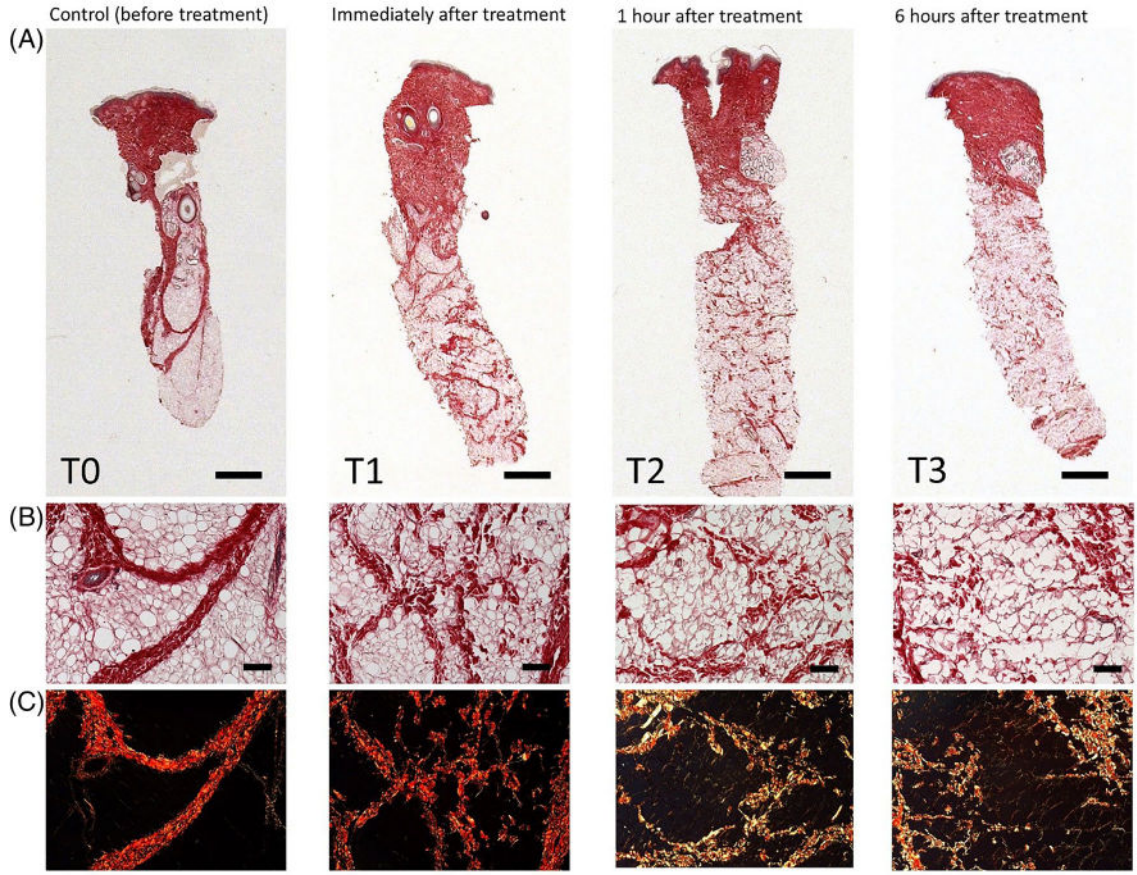

FIGURE 1 A, Skin biopsy samples at very low magnification, sectioned longitudinally and perpendicularly to the skin surface, Picrosirius red stained. Bars: 1 mm. B, Higher magnification of subcutaneous adipose tissue at the common light microscope. Interlobular septa constituted by fibrous connective tissue proper, delimiting adipose tissue lobules, appear intensely stained by Picrosirius red. Remark, as in, A, the progressive reduction of septa thickness. Bars: 100 μm. C, The same microscopic fields of, B, observed at the same light microscope, but using suitable set filters for circularly polarized light. Collagen fibers, whose birefringence is enhanced by the Picrosirius red staining, appear bright and colored on the black background (adipocytes are not birefringent). The color at T0 is red. At T1 (immediately after treatment), T2 (1 hour after), and T3 (6 hours after), some spots yellow and yellow/green are detectable in the progressively thinner and fragmented interlobular septa

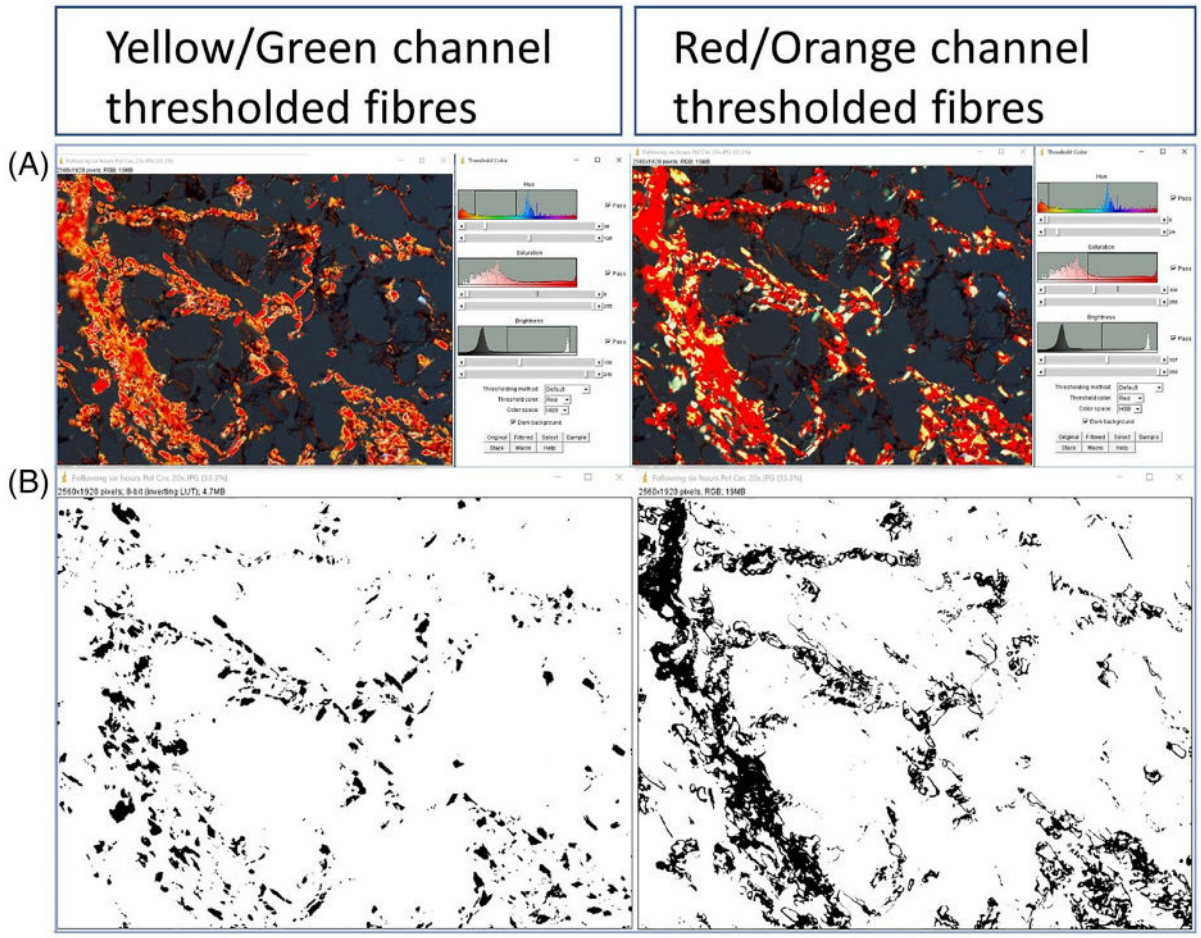

FIGURE 2 An example of how to extract by thresholding, from images obtained following Picrosirius red staining and circularly polarized light with suitable filters, collagen fibers of different nature through different colors. A, The small diagrams attached to microphotographs report the thresholds used for separating the Yellow/Green and the Red/Orange fibers. In B, the binary images suitable for measurements, obtained after thresholding, are reported

suitable thresholds (Yellow/Green, collagen III and Orange/Red, collagen I). The threshold areas corresponding to fibers selected in each one of the two bands are selected in the binary images as black structures (Figure 2B) and measured as percentage compared to the full frame reference area. Computerized morphometric analysis for the evaluation of collagen I and collagen III in interlobular septa was performed and the results of the different collagen contents are reported in Figure 3. It is evident, following MW treatment, the significant decrease of big fibrous collagen I and the respective increase of thin fibrillar collagen III.

4 | DISCUSSION

Owing to our use of the dye Sirius red, Picrosirius red is intensely and specifically staining collagen and enhances collagen birefringence.[5] Other authors demonstrated the advantages of this technique compared to traditional methods in studying the differential distribution of the structurally distinct collagen types.[6,8-11] Some authors have reported collagenolysis with related stimulation of new collagen synthesis, into vesical prolapse lesions.[12]

Due to the variability of the traditional trichrome staining which do not always stain collagen fibers with the same color and some fibers do not stain at all,[11] in contrast, the enhancement of collagen's natural birefringence by Picrosirius red stain reveals more collagen than can be seen after trichrome staining. With this method, even fine collagen fibers can also be identified due to their enhanced birefringence.[11] The enhancement of birefringence is highly specific for collagen, due to the fact that many Sirius red dye molecules (5 nm in size) link parallel to the long axis of each collagen molecule, both thick and very thin as single or few tropocollagen molecules[12] so increasing anisotropy and collagen birefringence.

In our study, we used circularly polarized light rather linear polarized light. The advantage of this choice is that all collagen fibers appear bright regardless of their orientation within the section plane,[7,11] permitting a reliable quantitative analysis of the whole collagen content. Owing to the different colors observed, Red/Orange or Yellow/Green, this is due to the degree of polymerization and packing of collagen molecules and their 3D organization. Big bundles of highly packed collagen molecules (Red/Orange) or thin bundles of few molecules of collagen (Yellow/Green), are reflecting

FIGURE 3 A,B, Reporting the results of measurements of the content (%) in the interlobular septa of collagen I (red columns) compared to the content (%) of collagen III (green columns) at T0 (control), T1 (immediately after treatment), T2 (1 hour after), and T3 (6 hours after) expressed as mean value ± SD. The significance level was <.01

Percentages content of Collagen I vs Collagen III

	Red/Orange Collagen I (old)	Yellow/Green Collagen III (newly formed)
T0 Control	13,01	0,23
T1 Immediately after	10,69	1,28
T2 1 hour	8,91	3,90
T3 6 hours	6,85	4,98

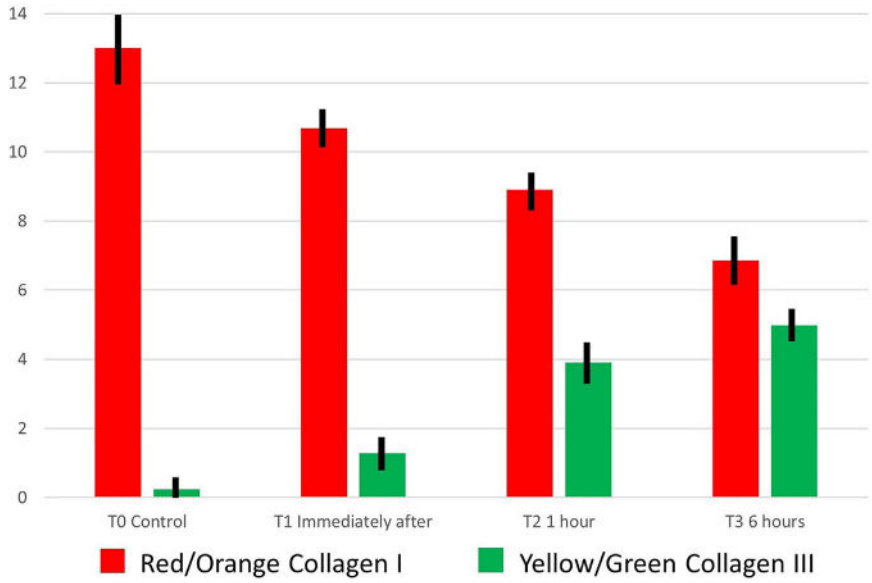

distinct patterns of physical aggregation and the different contents of mature, old collagen (collagen I), and immature, newly formed collagen (collagen III).[8,12-14]

Morphological and morphometric data following treatment, obtained using Picrosirius red staining and circularly polarized microscopy, represented by a decrease of big Red/Orange fibers and an increase of thin green/yellow fibers, realistically is representing a strong support to the activation of a remodeling mechanism of the interlobular septa, with consequent reduction of compacted fibrous collagen bundles.[11,15-17] An important role in the renewal of collagen is realistically played by metalloproteinases, a family of matrix enzymes Zn-dependent, as MMP-2, well known as interstitial collagenase.[18] MMP-2 is converted from the inactive form to the active molecular form in a very short time, due to an energetic charge from external MW application. This conversion is starting the digestion of the old fibrotic bundles of collagen I, preparing the extracellular matrix of the connective tissue to the renewal of fibrillar components, stimulating fibroblasts to the synthesis of new native collagen, defining a new balance rich in finely fibrillar collagen III. A similar mechanism has been demonstrated following energy transfer, in that case by fractional CO_2 laser treatment of atrophic vaginal mucosa, where an increase of MMP-2 active form corresponded to an increase of finely fibrillar collagen III in the mucosal connective tissue.[19] This example constitutes a significant indication of degradation of the old collagen due to active MMP-2 and production of a new collagen, as the result of a remodeling mechanism occurring in the regenerative process of the connective tissue. These results are in some respect similar to those obtained following photobiomodulation energy transfer in the skin,[13] even if in that paper, it was used a photosensitizer and the evaluation of the effects was made after a longer time.

Many other factors could be realistically involved in these mechanisms and have to be investigated, as the release of cytokines, the role of heat shock proteins, often responsible for the response of tissues to energy transfer.

5 | CONCLUSIONS

Our morphologic data have shown significant evidence of the reduction of compacted fibrous connective tissue constituting interlobular septa in the SAT following MW irradiation. Our findings support the effectiveness of the new device treatment not only for the reduction of subcutaneous fat, but also for cellulite and related dimpled, bumpy, or orange peel-like skin.

ORCID

Mohammad Jafferany https://orcid.org/0000-0001-6358-9068
Julia Sigova https://orcid.org/0000-0002-5571-0929
Torello Lotti https://orcid.org/0000-0003-0840-1936

REFERENCES

1. Asan NB, Noreland D, Hassan E, et al. Intra-body microwave communication through adipose tissue. *Healthc Technol Lett*. 2017;4(4):115-121. https://doi.org/10.1049/htl.2016.0104.
2. Zerbinati N, d'Este E, Cornaglia AI, et al. New system delivering microwaves energy for inducing subcutaneous fat reduction: in vivo histological and ultrastructural evidence. *Open Access Maced J Med Sci*. 2019;7(18):2991-2997. https://doi.org/10.3889/oamjms.2019.778.eCollection2019Sep30.
3. Mayo Clinic (2018). Available from https://www.mayoclinic.org/diseases-conditions/cellulite
4. Omi T, Sato S, Kawana S. Ultrastructural assessment of cellulite morphology: clues to a therapeutic strategy? *Laser Ther*. 2013;22(2):131-136. https://doi.org/10.3136/islsm.22131.
5. Puchtler H, Waldrop FS, Valentine LS. Polarization microscopic studies of connective tissue stained with picrosirius red FBA. *Beitr Path*. 1973;150:174-187.
6. Junqueira LC, Bignolas G, Brentani RR. Picrosirius staining plus polarization microscopy, a specific method for collagen detection in tissue sections. *Histochem J*. 1979;11:447-455.
7. Frohlich MW. Birefringent objects visualized by circular polarization microscopy. *Stain Technol*. 1986;61:139-143.
8. Junqueira LC, Cossermelli W, Brentani R. Differential staining of collagens type I, II and III by sirius red and polarization microscopy. *Arch Histol Jap*. 1978;41:267-274.
9. Dayan D, Hiss Y, Hirshberg A, Bubis JJ, Wolman M. Are the polarization colors of picrosirius red-stained collagen determined only by the diameter of the fibers? *Histochemistry*. 1989;93:27-29.
10. Whittaker P, Kloner RA, Boughner DR, Pickering JG. Quantitative assessment of myocardial collagen with picrosirius red staining and circularly polarized light. *Basic Res Cardiol*. 1994;89:397-410.
11. Whittaker P. Polarized light microscopy in biomedical research. *Microsc Anal*. 1995;33:13-15.
12. Borges LF, Gutierrez PS, Marana HR, Taboga SR. Picrosirius-polarization staining method as an efficient histopathological tool for collagenolysis detection in vesical prolapse lesions. *Micron*. 2007;38:580-583.
13. de Jesus PD, Saeki SI, Tedesco AC. An ex vivo study of photobiostimulation in the treatment of skin pathologies. *J Biophotonics*. 2016;9:1189-1198. https://doi.org/10.1002/jbio.201500288.
14. Zerbinati N, Calligaro A. Calcium hydroxylapatite treatment of human skin: evidence of collagen turnover through picrosirius red staining and circularly polarized microscopy. *Clin Cosmet Investig Dermatol*. 2018;11:29-35. https://doi.org/10.2147/CCID.S143015.
15. Vidal BC, Mello ML, Pimentel ER. Polarization microscopy and microspectrophotometry of Sirius red, Picrosirius and chlorantine fast red aggregates and of their complexes with collagen. *Histochem J*. 1982;14:857-878. https://doi.org/10.1007/BF01005229.
16. Whittaker P, Boughner DR, Kloner RA. Analysis of healing after myocardial infarction using polarized light microscopy. *Am J Pathol*. 1989;134:879-893.
17. Rich L, Whittaker P. Collagen and picrosirius red staining: a polarized light assessment of fibrillar hue and spatial distribution. *Braz J Morphol Sci*. 2005;22:97-104.
18. Aimes RT, Quigley JP. Matrix metalloproteinase-2 is an interstitial collagenase. Inhibitor-free enzyme catalyzes the cleavage of collagen fibrils and soluble native type I collagen generating the specific 3/4- and 1/4-length fragments. *J Biol Chem*. 1995;270:5872-5876. https://doi.org/10.1074/jbc.270.11.5872.
19. Salvatore S, França K, Lotti T, et al. Early regenerative modifications of human postmenopausal atrophic vaginal mucosa following fractional CO2 laser treatment. *Open Access Maced J Med Sci*. 2018;6(1):6-14. https://doi.org/10.3889/oamjms.2018.058.

How to cite this article: Zerbinati N, d'Este E, Farina A, et al. Remodeling of collagen constituting interlobular septa of subcutaneous adipose tissue following microwaves application. *Dermatologic Therapy*. 2020;e13362. https://doi.org/10.1111/dth.13362